

Thermodynamic Properties of Brucite Determined by Solubility Studies and Their Significance to Nuclear Waste Isolation

Yongliang Xiong

Received: 29 November 2007 / Accepted: 16 June 2008 / Published online: 11 July 2008
© Springer Science+Business Media B.V. 2008

Abstract Solubility experiments were conducted for the dissolution reaction of brucite, $\text{Mg}(\text{OH})_2(\text{cr})$: $\text{Mg}(\text{OH})_2(\text{cr}) + 2\text{H}^+ = \text{Mg}^{2+} + 2\text{H}_2\text{O}$. Experiments were conducted from undersaturation in deionized (DI) water and 0.010–4.4 m NaCl solutions at 22.5°C. In addition, brucite solubility was measured from supersaturation in an experiment in which brucite was precipitated via dropwise addition of 0.10 m NaOH into a 0.10 m MgCl_2 solution also at 22.5°C. The attainment of the reversal in equilibrium was demonstrated in this study. The solubility constant at 22.5°C at infinite dilution calculated from the experimental results from the direction of supersaturation by using the specific interaction theory (SIT) is: $\log K_s^\circ = 17.2 \pm 0.2$ (2σ) with a corresponding value of 17.0 ± 0.2 (2σ) when extrapolated to 25°C. The dimensionless standard chemical potential (μ°/RT) of brucite derived from the solubility data in 0.010 m to 4.4 m NaCl solutions from undersaturation extrapolated to 25°C is -335.76 ± 0.45 (2σ), with the corresponding Gibbs free energy of formation of brucite, $\Delta_f G_{298.15, \text{brucite}}^\circ$, being -832.3 ± 1.1 (2σ) kJ mol^{-1} . In combination with the auxiliary thermodynamic data, the $\log K_s^\circ$ is calculated to be 17.1 ± 0.2 (2σ), based on the above Gibbs free energy of formation for brucite. This study recommends an average value of 17.05 ± 0.2 in logarithmic unit as solubility constant of brucite at 25°C, according to the values from both supersaturation and undersaturation.

Keywords Solubility studies · Specific interaction theory (SIT) · Pitzer equations · Solubility constants · Hydromagnesite · Nuclear waste isolation

Sandia National Laboratories is a multiprogram laboratory operated by Sandia Corporation, a Lockheed Martin Company, for the United States Department of Energy's National Nuclear Security Administration under Contract DE-AC04-94AL85000.

Y. Xiong (✉)
Sandia National Laboratories (SNL), Carlsbad Programs Group,
4100 National Parks Highway, Carlsbad, NM 88220, USA
e-mail: yxiong@sandia.gov

1 Introduction

An accurate knowledge of the thermodynamic properties of brucite ($\text{Mg}(\text{OH})_2$) is important for nuclear waste isolation. Brucite has become significant to waste isolation projects owing to its use as engineered barriers for nuclear waste repositories. Crystalline MgO , which hydrates rapidly to brucite, is the only engineered barrier certified by the US Environmental Protection Agency (EPA) for the Waste Isolation Pilot Plant (WIPP) located near Carlsbad, New Mexico, USA (e.g., Krumhansl et al. 2000; Xiong and Snider 2003). An $\text{Mg}(\text{OH})_2$ -based engineered barrier is also proposed for the German Asse salt mine repository (Schüssler et al. 2002). The geochemical functions of the engineered barrier in the WIPP are (1) to consume CO_2 possibly produced by microbial degradation of organic materials in the waste and waste packages and (2) to buffer the pH and fugacity of CO_2 gas (f_{CO_2}) of the repository (Krumhansl et al. 2000; Xiong and Snider 2003). Experimental work at Sandia National Laboratories conducted at room temperature and atmospheric P_{CO_2} indicates that MgO first hydrates to brucite, which in turn is carbonated to form hydromagnesite (5424) ($\text{Mg}_5(\text{CO}_3)_4(\text{OH})_2 \cdot 4\text{H}_2\text{O}$) (Xiong and Snider 2003; Xiong and Lord 2008). Consequently, the thermodynamic properties of the brucite-hydromagnesite (5424) assemblage are of great significance to the performance assessment (PA) because actinide solubility is strongly affected by f_{CO_2} . In addition, PA is important to the demonstration of the long-term safety of nuclear waste repositories, as assessed by the use of probabilistic performance calculations.

A literature review of the thermodynamic properties of brucite shows that there is a substantial discrepancy in the values of $\Delta_f G_{298.15, \text{brucite}}^\circ$ reported in the literature. These values range from -831.4 (Harvie et al. 1984), -831.9 (Brown et al. 1996), -833.5 (Robie and Hemingway 1995), to -836.5 kJ mol^{-1} (Königsberger et al. 1999). Using the $\Delta_f G_{298.15, \text{hydromagnesite}(5424)}^\circ$ from Königsberger et al. (1999), the predicted $\log f_{\text{CO}_2}$ in equilibrium with the brucite-hydromagnesite assemblage (5424) would range from -5.96 ($\Delta_f G_{298.15, \text{brucite}}^\circ$ from Harvie et al. 1984) to -4.84 ($\Delta_f G_{298.15, \text{brucite}}^\circ$ from Königsberger et al. 1999). The above discussion shows that a much better constrained value for $\Delta_f G_{298.15, \text{brucite}}^\circ$ is required to accurately assess the role of brucite in nuclear waste repositories. For this reason, a series of solubility experiments involving brucite from the direction of undersaturation in DI water, and NaCl solutions ranging from 0.010 to 4.4 m (molality), were conducted at room temperature. In addition, in order to assess the reversal in equilibrium, one experiment was conducted from the direction of supersaturation with respect to brucite. These experiments were used to determine the solubility constant of brucite and derive new values of $\Delta_f G_{298.15, \text{brucite}}^\circ$ via the computer modeling. These results were initially summarized and reported in 2003 (Xiong 2003). In the meantime, Altmaier et al. (2003) also conducted a similar solubility study on brucite. However, all of their experiments were from the direction of undersaturation, and therefore, the attainment of the reversal in equilibrium was not demonstrated in their study, which is important to solubility studies, especially those at low temperatures. This communication reports the results obtained in this study. In light of this, the significance of the thermodynamic properties of brucite in nuclear waste isolation is demonstrated by performing calculations of important geochemical parameters such as $\log f_{\text{CO}_2}$.

2 Methodology

All materials (NaCl , $\text{MgCl}_2 \cdot 6\text{H}_2\text{O}$, $\text{Mg}(\text{OH})_2$, NaOH) used in this study are reagent grade from Fisher Scientific. Deionized (DI) water with $18.3 \text{ M}\Omega$ was produced by a *NANOpure*

Infinity Ultra Pure Water System from Barnstead. Degassed DI water was used for preparation of all starting solutions. The degassed DI water was obtained by bubbling high purity argon gas (purity 99.996%) from AIR GAS, inc., through DI water for at least 1 h, following a procedure similar to that described by Wood et al. (2002). Starting solutions were prepared such that the equilibrium solubility was approached from both under- and supersaturation with respect to brucite. For the undersaturated experiments, the starting solutions included DI water and NaCl solutions ranging from 0.010 to 4.4 m NaCl. The supersaturation experiment used a 0.10 m MgCl_2 starting solution.

All experiments were conducted at room temperature ($22.5 \pm 1.5^\circ\text{C}$). For each of the experiments undersaturated with respect to brucite, 5 g of $\text{Mg}(\text{OH})_2$ (cr) was placed into a 30-ml Oak Ridge centrifuge tube containing 30g of starting solution (NaCl solution or DI water). In order to determine the equilibrium brucite solubility from the direction of supersaturation, about 450 ml of 0.10 m MgCl_2 solution was placed in a 500 ml polyethylene bottle. Brucite was subsequently precipitated from the solution via dropwise addition of a 0.10 m NaOH solution. All experimental solutions (both under- and supersaturation) were placed on an INNOVA 2100 Platform Shaker (New Brunswick Scientific, Inc.) at a shaking speed of 140 rpm for the duration of the experiments.

At specific intervals, the pH of each experimental solution was measured with an Orion-Ross combination pH glass electrode. Before each measurement, the pH meter was calibrated with three pH buffers (pH 4, 7, and 10). For solutions with ionic strengths higher than 0.10 m, the observed solution pH values were converted to hydrogen-ion concentrations (pCH) in molality using a correction factor, A (see below).

The relation between the pH electrode reading (pH_{ob}) and pCH can be expressed as (Rai et al. 1995):

$$\text{pCH} = \text{pH}_{\text{ob}} + A \quad (1)$$

The linear relation between A values and concentrations for NaCl solutions for various Orion-Ross combination electrodes obtained by Rai et al. (1995) is expressed as:

$$A = 0.159X \quad (2)$$

where X is the NaCl concentration in molality. This expression is valid for NaCl solutions up to 6.0 m in concentration. They also performed a study to evaluate the dependence of the A values on an individual electrode by using a number of different Orion-Ross electrodes. They concluded that there is no significant difference in A values for different electrodes.

After a pH measurement was taken, certain amounts of solution were withdrawn from an experimental run. The solution was filtered using a 0.2 μm syringe filter. The filtered solution was then weighed and acidified with 0.5 ml of concentrated HNO_3 (TraceMetal grade from Fisher Scientific). The extracted solution was then diluted to 10 ml with DI water so that dissolved ΣMg^{2+} and Na^+ concentrations could be determined.

The chemical analyses of solutions were performed with a Perkin Elmer dual-view inductively coupled plasma-atomic emission spectrometer (ICP-AES) (Perkin Elmer DV 3300). Calibration blanks and standards were precisely matched with experimental matrices. The correlation coefficients of calibration curves in all measurements were better than 0.9995. The analytical precision is better than 1.00% in terms of the relative standard deviation (RSD) based on replicate analyses.

Solid phase identification was performed using a Bruker AXS, Inc., D8 Advance X-ray diffractometer (XRD) with a Sol-X detector. XRD patterns were collected using $\text{CuK}\alpha$

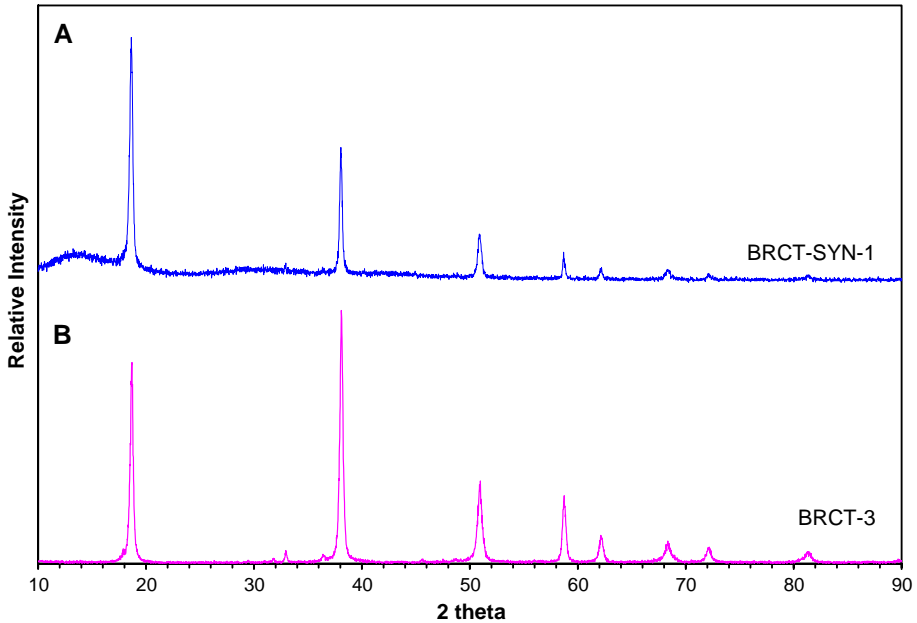


Fig. 1 Representative XRD patterns of brucite after the experimental runs. **(a)** XRD patterns for the experimental run from supersaturation (BRCT-SYN-1) started with 0.1 m MgCl_2 . **(b)** XRD patterns for the experimental run from undersaturation (BRCT-3) in 0.1 m NaCl

radiation at a scanning rate of $1.33^\circ/\text{min}$ for a 2θ range of $10\text{--}90^\circ$. No new phase is observed (see representative XRD patterns in Fig. 1). The crystallite diameters of brucite were measured using a JEOL JSM-5900LV scanning electron microscope (SEM) with an energy dispersive spectroscopy (EDS) of the ThermoNORAN Vantage digital acquisition system.

3 Experimental Results

Results for the experimental runs starting with DI water are given in Table 1. Experimental results from the supersaturated run (0.10 m MgCl_2 starting solution) are tabulated in Table 2. All other experimental results are tabulated in Table 3. In Fig. 2, a plot of $\log m_{\Sigma\text{Mg}}/m_{\text{H}^+}$ versus time is shown for the 0.10 m NaCl experiment that approached equilibrium from undersaturation with respect to brucite. The plot in Fig. 2 also shows the results for the supersaturation experiment in which brucite was precipitated from a 0.10 m MgCl_2 solution. Because these two experimental runs have similar ionic strengths ($I = \sim 0.11$ m for the 0.10 m NaCl experiment; and $I = \sim 0.25$ m for the 0.10 m MgCl_2 experiment), the consistent results from these sets of experiments indicate that the reversal was attained after about 2,000 h (Fig. 2). This serves as the criterion for selecting experimental results to calculate the equilibrium constants and to do the modeling. The ionic strength of the experiment with the 0.10 m MgCl_2 solution from which brucite was precipitated by dropwise addition of 0.10 m NaOH was calculated using the Na and Mg concentrations determined by ICP-AES, and the original Cl concentration:

Table 1 Experimental results from the experiment BRCT-1 starting with deionized (DI) water

Experimental run number	Run time, hour	pH _{ob}	$m_{\text{Mg}^{2+}}$	I_m	$\log \gamma_{\text{Mg}^{2+}}$	$\log K^\circ$ ^b	
BRCT-1	701	10.04	3.31×10^{-3}	9.92×10^{-3}	-1.78×10^{-1}	N/A	
	890	10.12	3.34×10^{-3}	1.00×10^{-2}	-1.79×10^{-1}	N/A	
	1205	10.06	3.54×10^{-3}	1.06×10^{-2}	-1.84×10^{-1}	N/A	
	1633	9.98	2.41×10^{-3}	7.23×10^{-3}	-1.55×10^{-1}	N/A	
	1896	10.10	1.88×10^{-3}	5.63×10^{-3}	-1.39×10^{-1}	N/A	
	2377 ^a	10.15	2.03×10^{-3}	6.09×10^{-3}	-1.44×10^{-1}	17.46	
	2879 ^a	10.20	1.62×10^{-3}	4.85×10^{-3}	-1.30×10^{-1}	17.48	
	3217 ^a	10.09	1.67×10^{-3}	5.01×10^{-3}	-1.32×10^{-1}	17.27	
	3406 ^a	10.05	1.70×10^{-3}	5.10×10^{-3}	-1.33×10^{-1}	17.20	
	3550 ^a	10.03	1.74×10^{-3}	5.23×10^{-3}	-1.34×10^{-1}	17.17	
	3744 ^a	10.09	1.22×10^{-3}	3.66×10^{-3}	-1.14×10^{-1}	17.15	
	3913 ^a	10.01	1.26×10^{-3}	3.79×10^{-3}	-1.16×10^{-1}	17.01	
	4222 ^a	10.09	1.36×10^{-3}	4.09×10^{-3}	-1.20×10^{-1}	17.20	
	4730 ^a	10.01	1.49×10^{-3}	4.46×10^{-3}	-1.25×10^{-1}	17.07	
	4971 ^a	10.07	1.10×10^{-3}	3.29×10^{-3}	-1.09×10^{-1}	17.07	
	Average						17.2 ± 0.3 (2 σ) ^c
							17.0 ± 0.3 (2 σ) ^d

^a The solubility data in which the experimental time exceeded 2,000 h by using the criterion set by the reversal mentioned in the text are selected for calculation of solubility constants

^b Equilibrium constants at infinite dilution ($\log K^\circ$) are computed by using measured pH_{ob}, measured $m_{\text{Mg}^{2+}}$, and $\log \gamma_{\text{Mg}^{2+}}$ calculated from the Davies equation, assuming unity for activity of water and brucite. The measured pH_{ob} was not corrected because the ionic strength is very low

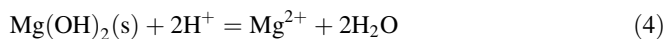
^c Value at 22.5°C

^d Value extrapolated to 25°C. In the extrapolation, all entropies are from Cox et al. (1989), and all heat capacities are from the compilation of Königsberger et al. (1999)

$$I_m = \frac{1}{2} (2^2 \times m_{\text{Mg}} + 1^2 \times m_{\text{Na}} + 1^2 \times m_{\text{Cl}}) \quad (3)$$

In order to obtain thermodynamic properties for brucite from the experimental results discussed above, the results from the supersaturated experiment (Table 2) were extrapolated to infinite dilution using the Specific Interaction Theory (SIT) interaction coefficients estimated by Xiong (2006).

The results obtained from the extrapolations using the SIT model to infinite dilution are the equilibrium constants for the brucite dissolution reaction:



The extrapolation to infinite dilution for the reaction Eq. 4 by using the SIT model is given by:

$$\log K_s^\circ = \log Q - 2D + \varepsilon(\text{Mg}^{2+}, \text{Cl}^-)I_m - 2\varepsilon(\text{H}^+, \text{Cl}^-)I_m + 2 \log a_{\text{H}_2\text{O}} \quad (5)$$

where $\log Q$ is an equilibrium quotient for the reaction given by Eq. 4 at a given ionic strength; $\varepsilon(\text{Mg}^{2+}, \text{Cl}^-)$ and $\varepsilon(\text{H}^+, \text{Cl}^-)$ are the interaction coefficients of the

Table 2 Experimental results from the experimental run BRCT-SYN-1 in which brucite was precipitated from 0.1 m MgCl₂ solution by dropwise addition of 0.1 m NaOH

Run time, hour	m_{Na^+}	pH _{ob}	m_{H^+}	$m_{\text{Mg}^{2+}}$	I_m	log Q	log $K^{\circ b}$
24	6.35×10^{-2}	9.34	4.41×10^{-10}	6.27×10^{-2}	2.57×10^{-1}	N/A	N/A
214	6.46×10^{-2}	9.32	4.61×10^{-10}	6.40×10^{-2}	2.60×10^{-1}	N/A	N/A
333	6.51×10^{-2}	9.27	5.18×10^{-10}	6.20×10^{-2}	2.56×10^{-1}	N/A	N/A
480	6.50×10^{-2}	9.37	4.11×10^{-10}	6.20×10^{-2}	2.57×10^{-1}	N/A	N/A
695	7.98×10^{-2}	9.37	4.11×10^{-10}	5.37×10^{-2}	2.47×10^{-1}	N/A	N/A
864	7.91×10^{-2}	9.24	5.55×10^{-10}	5.23×10^{-2}	2.44×10^{-1}	N/A	N/A
1173	7.83×10^{-2}	9.33	4.51×10^{-10}	5.36×10^{-2}	2.46×10^{-1}	N/A	N/A
1681	8.42×10^{-2}	9.25	5.42×10^{-10}	5.24×10^{-2}	2.47×10^{-1}	N/A	N/A
1922	7.78×10^{-2}	9.30	4.83×10^{-10}	5.16×10^{-2}	2.42×10^{-1}	N/A	N/A
2426 ^a	7.93×10^{-2}	9.27	5.18×10^{-10}	5.20×10^{-2}	2.44×10^{-1}	17.34	17.03
5447 ^a	$7.20 \times 10^{-2 c}$	9.22	5.81×10^{-10}	6.40×10^{-2}	2.64×10^{-1}	17.32	17.02
8833 ^a	$8.39 \times 10^{-2 c}$	9.40	3.84×10^{-10}	5.80×10^{-2}	2.58×10^{-1}	17.60	17.34
9169 ^a	$8.34 \times 10^{-2 c}$	9.38	4.02×10^{-10}	5.83×10^{-2}	2.58×10^{-1}	17.56	17.30
10,776 ^a	$1.15 \times 10^{-1 c}$	9.48	3.19×10^{-10}	4.27×10^{-2}	2.43×10^{-1}	17.62	17.36
11,642 ^a	$1.12 \times 10^{-1 c}$	9.42	3.66×10^{-10}	4.39×10^{-2}	2.44×10^{-1}	17.51	17.25
12,047 ^a	$1.18 \times 10^{-1 c}$	9.42	3.66×10^{-10}	4.12×10^{-2}	2.41×10^{-1}	17.49	17.23
12,284 ^a	$1.13 \times 10^{-1 c}$	9.42	3.66×10^{-10}	4.33×10^{-2}	2.43×10^{-1}	17.51	17.25
13,391 ^a	$1.14 \times 10^{-1 c}$	9.39	3.93×10^{-10}	4.31×10^{-2}	2.43×10^{-1}	17.45	17.19
14,304 ^a	$1.12 \times 10^{-1 c}$	9.39	3.93×10^{-10}	4.41×10^{-2}	2.44×10^{-1}	17.46	17.20
26,692 ^a	$1.10 \times 10^{-1 c}$	9.29	4.94×10^{-10}	4.52×10^{-2}	2.45×10^{-1}	17.27	17.01

Table 2 continued

Run time, hour	m_{Na^+}	pH _{obs}	m_{H^+}	$m_{\text{Mg}^{2+}}$	I_m	log Q	log K^{c} ^b
35,830 ^d	$8.14 \pm 0.06 \times 10^{-2}$	9.38	4.02×10^{-10}	$4.94 \pm 0.11 \times 10^{-2}$	2.40×10^{-1}	17.49	17.23
36,337 ^d	$8.37 \pm 0.02 \times 10^{-2}$	9.36	4.21×10^{-10}	$4.84 \pm 0.04 \times 10^{-2}$	2.39×10^{-1}	17.44	17.18
Average						17.5 ± 0.2 (2 σ) ^d	17.2 ± 0.2 (2 σ) ^d 17.0 ± 0.2 (2 σ) ^e

^a The solubility data in which the experimental time exceeded 2,000 h by using the criterion set by the reversal mentioned in the text are selected for calculation of solubility constants

^b Equilibrium constants at infinite dilution are obtained by using the SIT model for extrapolation based on the interaction coefficients, $\epsilon(\text{Mg}^{2+}, \text{Cl}^-)$, and $\epsilon(\text{H}^+, \text{Cl}^-)$ from Xiong (2006)

^c Calculated from charge balance equation

^d Values at 22.5°C

^e Value extrapolated to 25°C. In the extrapolation, all entropies are from Cox et al. (1989), and all heat capacities are from the compilation of Königsberger et al. (1999)

Table 3 Experimental results from the experimental runs from the direction of undersaturation in various NaCl solutions from 0.010 to 4.4 m

Experimental run number	Medium	Run time, h	pH _{ob}	m_{H^+}	$m_{Mg^{2+}}$	m_{OH^-}
BRCT-2-1F	0.010 m NaCl	702	10.05	8.88×10^{-11}	3.44×10^{-3}	1.14×10^{-4}
BRCT-2-2F		890	10.13	7.39×10^{-11}	3.63×10^{-3}	1.38×10^{-4}
BRCT-2-3F		1205	10.07	8.48×10^{-11}	3.70×10^{-3}	1.20×10^{-4}
BRCT-2-4F		1633	10.05	8.88×10^{-11}	2.41×10^{-3}	1.14×10^{-4}
BRCT-2-5F		1896	10.03	9.30×10^{-11}	2.50×10^{-3}	1.09×10^{-4}
BRCT-2-6F		2377 ^a	10.08	8.29×10^{-11}	2.62×10^{-3}	1.23×10^{-4}
BRCT-2-7F		2879 ^a	10.12	7.56×10^{-11}	2.03×10^{-3}	1.34×10^{-4}
BRCT-2-8F		3217 ^a	10.05	8.88×10^{-11}	2.09×10^{-3}	1.14×10^{-4}
BRCT-2-9F		3406 ^a	10.00	9.96×10^{-11}	2.15×10^{-3}	1.02×10^{-4}
BRCT-2-10F		3550 ^a	10.06	8.68×10^{-11}	2.23×10^{-3}	1.17×10^{-4}
BRCT-2-11F		3744 ^a	10.08	8.29×10^{-11}	1.45×10^{-3}	1.23×10^{-4}
BRCT-2-12F		3913 ^a	10.00	9.96×10^{-11}	1.53×10^{-3}	1.02×10^{-4}
BRCT-2-13F		4222 ^a	10.07	8.48×10^{-11}	1.66×10^{-3}	1.20×10^{-4}
BRCT-2-14F		4730 ^a	9.98	1.04×10^{-10}	1.78×10^{-3}	9.74×10^{-5}
BRCT-2-15F		4791 ^a	10.03	9.30×10^{-11}	1.37×10^{-3}	1.09×10^{-4}
BRCT-3-1F	0.10 m NaCl	702	10.08	8.02×10^{-11}	$4.18 \pm 0.10 \times 10^{-3}$ b	2.07×10^{-4}
BRCT-3-2F		890	10.22	5.81×10^{-11}	$4.32 \pm 0.06 \times 10^{-3}$ b	2.86×10^{-4}
BRCT-3-3F		1205	10.12	7.31×10^{-11}	$4.61 \pm 0.04 \times 10^{-3}$ b	2.27×10^{-4}
BRCT-3-4F		1633	10.09	7.84×10^{-11}	$3.04 \pm 0.10 \times 10^{-3}$ b	2.12×10^{-4}
BRCT-3-5F		1896	10.04	8.79×10^{-11}	2.96×10^{-3}	1.89×10^{-4}
BRCT-3-6F		2401 ^a	10.14	6.98×10^{-11}	3.21×10^{-3}	2.38×10^{-4}
BRCT-3-7F		2879 ^a	10.20	6.08×10^{-11}	2.17×10^{-3}	2.73×10^{-4}
BRCT-3-8F		3217 ^a	10.09	7.84×10^{-11}	2.28×10^{-3}	2.12×10^{-4}
BRCT-3-9F		3406 ^a	10.05	8.59×10^{-11}	2.29×10^{-3}	1.93×10^{-4}
BRCT-3-10F		3550 ^a	10.12	7.31×10^{-11}	2.38×10^{-3}	2.27×10^{-4}
BRCT-3-11F		3744 ^a	10.14	6.98×10^{-11}	1.66×10^{-3}	2.38×10^{-4}
BRCT-3-12F		3913 ^a	10.06	8.39×10^{-11}	1.72×10^{-3}	1.98×10^{-4}
BRCT-3-13F		4222 ^a	10.13	7.14×10^{-11}	1.83×10^{-3}	2.32×10^{-4}
BRCT-3-14F		4730 ^a	10.04	8.79×10^{-11}	1.88×10^{-3}	1.89×10^{-4}
BRCT-3-15F		4971 ^a	10.10	7.66×10^{-11}	1.38×10^{-3}	2.17×10^{-4}
BRCT-4-1F	1.0 m NaCl	702	10.00	6.89×10^{-11}	5.48×10^{-3}	2.77×10^{-4}
BRCT-4-2F		890	10.07	5.86×10^{-11}	5.58×10^{-3}	3.26×10^{-4}
BRCT-4-3F		1205	10.03	6.43×10^{-11}	6.01×10^{-3}	2.97×10^{-4}
BRCT-4-4F		1633	9.83	1.02×10^{-10}	4.19×10^{-3}	1.88×10^{-4}
BRCT-4-5F		1896	9.78	1.14×10^{-10}	4.37×10^{-3}	1.67×10^{-4}
BRCT-4-6F		2377 ^a	9.84	9.95×10^{-11}	4.38×10^{-3}	1.92×10^{-4}
BRCT-4-7F		2879 ^a	9.98	7.21×10^{-11}	3.10×10^{-3}	2.65×10^{-4}
BRCT-4-8F		3216 ^a	9.94	7.91×10^{-11}	3.29×10^{-3}	2.42×10^{-4}
BRCT-4-9F		3406 ^a	9.84	9.95×10^{-11}	3.32×10^{-3}	1.92×10^{-4}
BRCT-4-10F		3550 ^a	9.89	8.87×10^{-11}	3.46×10^{-3}	2.15×10^{-4}
BRCT-4-11F		3744 ^a	9.98	7.21×10^{-11}	2.11×10^{-3}	2.65×10^{-4}

Table 3 continued

Experimental run number	Medium	Run time, h	pH _{ob}	m_{H^+}	$m_{\text{Mg}^{2+}}$	m_{OH^-}
BRCT-4-12F		3913 ^a	9.90	8.67×10^{-11}	2.26×10^{-3}	2.20×10^{-4}
BRCT-4-13F		4222 ^a	9.94	7.91×10^{-11}	$2.44 \pm 0.00 \times 10^{-3}$ ^b	2.42×10^{-4}
BRCT-4-14F		4730 ^a	9.86	9.51×10^{-11}	2.71×10^{-3}	2.00×10^{-4}
BRCT-4-15F		4971 ^a	9.94	7.91×10^{-11}	2.06×10^{-3}	2.42×10^{-4}
BRCT-5-1F	2.1 m NaCl	93	9.78	7.73×10^{-11}	4.70×10^{-3}	1.93×10^{-4}
BRCT-5-2F		309	9.72	8.88×10^{-11}	6.69×10^{-3}	1.68×10^{-4}
BRCT-5-3F		480	9.73	8.67×10^{-11}	4.51×10^{-3}	1.72×10^{-4}
BRCT-5-4F		787 ^{ra>}	9.71	9.08×10^{-11}	5.21×10^{-3}	1.64×10^{-4}
BRCT-5-5F		1295	9.65	1.04×10^{-10}	5.32×10^{-3}	1.43×10^{-4}
BRCT-5-6F		1536	9.71	9.08×10^{-11}	3.91×10^{-3}	1.64×10^{-4}
BRCT-5-7F		2040 ^a	9.67	9.96×10^{-11}	4.14×10^{-3}	1.50×10^{-4}
BRCT-5-8F		2611 ^a	9.54	1.34×10^{-10}	4.27×10^{-3}	1.11×10^{-4}
BRCT-5-9F		3047 ^a	9.66	1.02×10^{-10}	3.21×10^{-3}	1.46×10^{-4}
BRCT-5-10F		3311 ^a	9.56	1.28×10^{-10}	3.48×10^{-3}	1.16×10^{-4}
BRCT-5-11F		5063 ^a	9.66	1.02×10^{-10}	3.69×10^{-3}	1.46×10^{-4}
BRCT-6-1F	3.2 m NaCl	93	9.71	6.04×10^{-11}	3.64×10^{-3}	1.66×10^{-4}
BRCT-6-2F		309	9.60	7.78×10^{-11}	5.49×10^{-3}	1.29×10^{-4}
BRCT-6-3F		480	9.58	8.15×10^{-11}	4.19×10^{-3}	1.23×10^{-4}
BRCT-6-4F		787	9.59	7.96×10^{-11}	4.67×10^{-3}	1.26×10^{-4}
BRCT-6-5F		1295	9.54	8.93×10^{-11}	5.11×10^{-3}	1.12×10^{-4}
BRCT-6-6F		1536	9.57	8.34×10^{-11}	3.63×10^{-3}	1.20×10^{-4}
BRCT-6-7F		2040 ^a	9.53	9.14×10^{-11}	3.92×10^{-3}	1.10×10^{-4}
BRCT-6-8F		2611 ^a	9.39	1.26×10^{-10}	3.64×10^{-3}	7.94×10^{-5}
BRCT-6-9F		3047 ^a	9.49	1.00×10^{-10}	2.94×10^{-3}	1.00×10^{-4}
BRCT-6-10F		3311 ^a	9.44	1.12×10^{-10}	3.13×10^{-3}	8.91×10^{-5}
BRCT-6-11F		5063 ^a	9.66	6.78×10^{-11}	3.32×10^{-3}	1.48×10^{-4}
BRCT-7-1F	4.4 m NaCl	94	9.63	4.70×10^{-11}	3.62×10^{-3}	1.35×10^{-4}
BRCT-7-2F		309	9.52	6.06×10^{-11}	5.28×10^{-3}	1.04×10^{-4}
BRCT-7-3F		480	9.47	6.80×10^{-11}	4.17×10^{-3}	9.32×10^{-5}
BRCT-7-4F		787	9.50	6.35×10^{-11}	4.66×10^{-3}	9.98×10^{-5}
BRCT-7-5F		1295	9.45	7.12×10^{-11}	5.04×10^{-3}	8.90×10^{-5}
BRCT-7-6F		1536	9.47	6.80×10^{-11}	3.21×10^{-3}	9.32×10^{-5}
BRCT-7-7F		2040 ^a	9.42	7.63×10^{-11}	3.54×10^{-3}	8.30×10^{-5}
BRCT-7-8F		2611 ^a	9.28	1.05×10^{-10}	3.62×10^{-3}	6.02×10^{-5}
BRCT-7-9F		3047 ^a	9.38	8.37×10^{-11}	2.81×10^{-3}	7.57×10^{-5}
BRCT-7-10F		3311 ^a	9.33	9.39×10^{-11}	2.90×10^{-3}	6.75×10^{-5}
BRCT-7-11F		5063 ^a	9.15	1.42×10^{-10}	8.87×10^{-3}	4.46×10^{-5}

^a Experimental data employed for NONLIN modeling to derive the dimensionless chemical potential

^b Replicate analyses

Brønsted-Guggenheim-Scatchard specific interaction theory recommended by Xiong (2006); $a_{\text{H}_2\text{O}}$ is activity of water; and D is the Debye-Hückel term.

The Debye-Hückel term is given by:

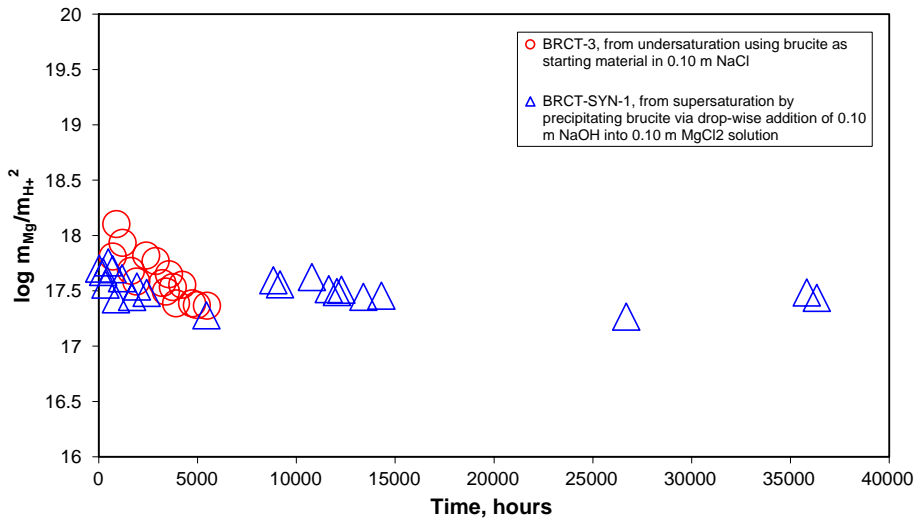


Fig. 2 A plot showing the attainment of reversal in experiments starting from both undersaturation and supersaturation

$$D = \frac{A_\gamma \sqrt{I_m}}{1 + \rho \sqrt{I_m}} \quad (6)$$

where A_γ is the Debye-Hückel slope for the activity coefficient (from Helgeson and Kirkham 1974); and ρ is the minimum distance of approach between ions, which is taken as 1.5 (Ciavatta 1980).

The activity of water is calculated from the expression (e.g., Guillaumont et al. 2003):

$$\log a_{\text{H}_2\text{O}} = \frac{-\phi \sum_k m_k}{\ln(10) \times 55.51} \quad (7)$$

where ϕ is the osmotic coefficient of the solution and the summation is taken over all solute species k with molality m_k in the solution. For a 1:1 electrolyte in which the contributions from all minor species have been ignored, Eq. 7 can be simplified to:

$$\log a_{\text{H}_2\text{O}} = \frac{-2 \times m_{\text{NX}} \times \phi}{\ln(10) \times 55.51} \quad (8)$$

For calculations using the experimental results of the 0.10 m MgCl_2 solution, the osmotic coefficient is taken from Rard and Miller (1981).

The dimensionless standard chemical potentials (μ°/RT) of brucite were derived from the solubility data from a wide range of ionic strengths in 0.010 to 4.4 m NaCl solutions (Table 3) from undersaturation by using the computer code NONLIN (Felmy 1990; Babb et al. 1996), which employs the Pitzer equations. Then, the dimensionless standard chemical potential of brucite obtained via the NONLIN modeling can be converted to the standard Gibbs free energy of formation of brucite ($\Delta_f G$). Finally, these values can be used in conjunction with the μ°/RT or $\Delta_f G$ values for each of the aqueous species in Eq. 4 to calculate the solubility constant of brucite. The Pitzer interaction parameters from Harvie et al. (1984) and dimensionless standard chemical potentials from Robie et al. (1978) and

Table 4 Pitzer interaction parameters and dimensionless standard chemical potentials used in NONLIN modeling

Binary interaction parameters ^a				
i	j	$\beta^{(0)}$, kg mol ⁻¹	$\beta^{(1)}$, kg mol ⁻¹	C^ϕ , kg ² mol ⁻²
H ⁺	Cl ⁻	0.1775	0.2945	0.0008
Na ⁺	Cl ⁻	0.0765	0.2664	0.00127
Na ⁺	OH ⁻	0.0864	0.253	0.0044
Mg ²⁺	Cl ⁻	0.35235	1.6815	0.00519
Ternary interaction parameters ^a				
i	j	k	θ_{ij} , kg mol ⁻¹	Ψ_{ijk} , kg ² mol ⁻²
Na ⁺	H ⁺	Cl ⁻	0.036	-0.004
Na ⁺	Mg ²⁺	Cl ⁻	0.07	-0.012
H ⁺	Mg ²⁺	Cl ⁻	0.10	-0.011
OH ⁻	Cl ⁻	Na ⁺	-0.050	-0.006
Dimensionless standard chemical potentials (μ°/RT) ^b				
H ₂ O(l)			-96.415	
H ⁺			0	
Na ⁺			-106.485	
Mg ²⁺			-185.159	
Cl ⁻			-53.345	
OH ⁻			-63.982	

^a All binary and ternary interaction coefficients are taken from the compilation of the FMT database (Babb et al. 1996; Babb and Novak 1997), which is based on Harvie et al. (1984)

^b Dimensionless standard chemical potentials at 298.15 K are from Robie et al. (1978), and Harvie et al. (1984), which have been extrapolated to 295.65 K according to temperature dependence of Gibbs free energy (Eq. 9). In the extrapolation, all entropies are from Cox et al. (1989), and all heat capacities are from the compilation of Königsberger et al. (1999)

Harvie et al. (1984) used in the NONLIN modeling are listed in Table 4. The molal concentrations of H⁺, Na⁺, Mg²⁺, Cl⁻ and OH⁻ are used as inputs. Among these, m_{H^+} and $m_{Mg^{2+}}$ are measured values, whereas m_{Na^+} and m_{Cl^-} are the initial concentrations of the starting solutions. The OH⁻ concentrations are calculated by using the measured m_{H^+} and the dissociation quotients of water in NaCl solutions at 25°C (Busey and Mesmer 1978).

As the solubility measurements were conducted at 22.5°C (295.65 K), thermodynamic data are extrapolated to standard temperature, 298.15 K, by using the following equation for temperature dependence of Gibbs free energy, assuming constant entropy and heat capacity over this temperature range,

$$\Delta G_T^\circ = \Delta G_{298.15}^\circ - (T - 298.15)\Delta S_{298.15}^\circ + \int_{298.15}^T \Delta C_p^\circ dT - T \int_{298.15}^T \Delta C_p^\circ d \ln T \quad (9)$$

In extrapolations, all entropies are from Cox et al. (1989), and all heat capacities are from the compilation of Königsberger et al. (1999).

The results in Tables 2 and 5 suggest that the solubility constants calculated directly from the SIT model and from the dimensionless standard chemical potential obtained using

Table 5 Dimensionless standard chemical potentials and corresponding Gibbs free energies of formation for brucite derived from solubility data of this study from the direction of undersaturation in NaCl solutions by using NONLIN^a

Experimental data sets for modeling	$[\frac{\mu^\circ}{RT}]_{295.65, \text{brucite}}$	$[\frac{\mu^\circ}{RT}]_{298.15, \text{brucite}}$	$\Delta_f G_{298.15}^\circ, \text{brucite}$ kJ mol ⁻¹
BRCT-2-6F to BRCT-2-15F; BRCT-3-6F to BRCT-3-15F; BRCT-4-6F to BRCT-4-15F; BRCT-5-7F to BRCT-5-11F; BRCT-6-7F to BRCT-6-11F; BRCT-7-7F to BRCT-7-11F	-338.55 ± 0.45 (2 σ)	-335.76 ± 0.45 (2 σ) ^b	-832.3 ± 1.1 (2 σ) ^b
Mg(OH) ₂ (s) + 2H ⁺ = Mg ²⁺ + 2H ₂ O	$\log K_{s,298.15}^\circ = 17.1 \pm 0.2$ (2 σ) ^c		

^a The solubility data from the direction of undersaturation selected for the NONLIN modeling to derive the dimensionless standard chemical potential are those in which the experimental time exceeded 2,000 h by using the criterion set by the reversal mentioned in the text

^b Extrapolated to 298.15 K according to the temperature dependence of Gibbs free energy (Eq. 9). In the extrapolation, entropy is from Cox et al. (1989), and heat capacity is from the compilation of Königsberger et al. (1999)

^c The solubility constant is calculated from the derived average standard Gibbs free energy of formation of brucite in conjunction with the auxiliary data for Mg²⁺, H₂O(l) and H⁺ from Cox et al. (1989)

the NONLIN modeling of the solubility data in NaCl medium are in excellent agreement within the given uncertainty. In addition, the average solubility constant calculated from the experiment started with DI water by using the Davies equation (Table 1) is also consistent with the above results.

4 Discussions and Applications

The logarithmic solubility constant of brucite determined from the direction of supersaturation in this study is 17.0 ± 0.2 (2 σ). The Gibbs free energy of formation of brucite derived from the solubility data from the direction of undersaturation in NaCl medium is -832.3 ± 1.1 (2 σ) kJ mol⁻¹. The solubility constant calculated from the Gibbs free energy of formation of brucite in conjunction with the auxiliary data for Mg²⁺, H₂O(l) and H⁺ from Cox et al. (1989) is 17.1 ± 0.2 (2 σ). Therefore, the solubility constant obtained from the supersaturation experiment is consistent with that obtained from the experiments from undersaturation within the experimental uncertainty. According to the solubility constants from both supersaturation and undersaturation, an average value of 17.05 ± 0.2 in log unit is recommended as the solubility constant of brucite.

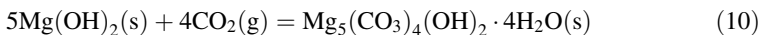
Based on SEM analyses, the crystallite diameters of brucite in the experiment from supersaturation range from 0.63 to 23 μm with an average of 5.2 ± 3.2 μm in accordance with 323 measurements. Similarly, the crystallite diameters of brucite in experiments from undersaturation range from 0.57 to 15 μm with an average of 5.4 ± 3.3 μm according to 63 measurements. In the study of the effect of particle size on surface energy of brucite, Hostetler (1963) concluded that the surface energy contribution to the solubility of brucite is “sensibly insignificant” when diameters of brucite grains are larger than ~ 0.15 μm . Therefore, the crystal sizes described above suggest that the surface energy contribution to the Gibbs free energy is insignificant in this study.

As mentioned before in the Introduction, Altmaier et al. (2003) also conducted a solubility study on brucite. All their experiments were from undersaturation without demonstration of the attainment of equilibrium. Instead, they treated the steady state

concentrations as equilibrium concentrations, and used the steady state concentrations to calculate the equilibrium constants. While the plots of $\log m_{\text{H}^+}$ as a function of experimental time were presented in their study, indicating the reach of the steady state in $\log m_{\text{H}^+}$, it is unclear about the concentrations of ΣMg as a function of time, as they were simply not presented. As the raw data were not provided in their study, it is unclear how the data were selected to calculate the equilibrium constants, and therefore it is impossible to do the re-calculations without the raw data. Nevertheless, it seems that the equilibrium constants (17.1 ± 0.2) at 22°C presented in their study are in fair agreement with those obtained in this study within the experimental uncertainty.

Altmaier et al. (2003) questioned the validity of the standard entropy of brucite ($S_{298.15, \text{brucite}}^\circ = 63.14 \text{ J K}^{-1} \text{ mol}^{-1}$) in the literature, which came from the original work of Giauque and Archibald (1937). This value is adopted by many thermodynamic tables. Their question is largely based on $\Delta_f H_{298.15, \text{brucite}}^\circ$ value of $-926.7 \text{ kJ mol}^{-1}$ calculated from enthalpy changes for the brucite solubility reaction determined by McGee and Hostetler (1977) and Brown et al. (1996). When combined with $\Delta_f G_{298.15, \text{brucite}}^\circ$ of $-831.9 \text{ kJ mol}^{-1}$ they mentioned, the above $\Delta_f H_{298.15, \text{brucite}}^\circ$ would lead to a much lower $S_{298.15, \text{brucite}}^\circ$ of $50.6 \text{ J K}^{-1} \text{ mol}^{-1}$. However, they did not mention that there is a body of calorimetric studies concerning the determination of $\Delta_f H_{298.15, \text{brucite}}^\circ$ as tabulated by Gurvich et al. (1994). The $\Delta_f H_{298.15, \text{brucite}}^\circ$ recommended by Gurvich et al. (1994) based on calorimetric studies is $-924.35 \pm 0.3 \text{ kJ mol}^{-1}$. By using $\Delta_f G_{298.15, \text{brucite}}^\circ$ of $-832.3 \text{ kJ mol}^{-1}$ suggested by this study, $S_{298.15, \text{brucite}}^\circ$ from Giauque and Archibald (1937), and the auxiliary data from CODATA (Cox et al. 1989), $\Delta_f H_{298.15, \text{brucite}}^\circ$ is calculated to be $-923.3 \pm 1.1 \text{ kJ mol}^{-1}$, which is consistent with the value adopted by Gurvich et al. (1994). Therefore, it can be concluded that the question of Altmaier et al. (2003) on $S_{298.15, \text{brucite}}^\circ$ of Giauque and Archibald (1937) is largely unfounded, when $\Delta_f H_{298.15, \text{brucite}}^\circ$ determined by calorimetric studies is considered.

As demonstrated by Xiong and Snider (2003), and Xiong and Lord (2008), the carbonation product of brucite at room temperature is hydromagnesite (5424). Therefore, the $\log f_{\text{CO}_2}$ in the repository would be controlled by the equilibrium buffer assemblage of brucite-hydromagnesite (5424), before hydromagnesite (5424) is converted to magnesite. According to the following reaction,



thus if the value of the Gibbs free energy of formation for brucite is changed, the predicted $\log f_{\text{CO}_2}$ will be different. In Table 6, the $\log f_{\text{CO}_2}$ predicted by using the Gibbs free energy of formation for brucite from this study and from Helgeson et al. (1978) are compared. In these above calculations, the Gibbs free energy of formation for hydromagnesite (5424) is taken from Robie and Hemingway (1995) and the other auxiliary data are taken from Cox et al. (1989). The results in Table 6 show that the $\log f_{\text{CO}_2}$, predicted by using the data for brucite from Helgeson et al. (1978) is higher than that predicted by using the data derived in this study by 0.65 orders of magnitude.

Since actinides can form strong aqueous complexes with carbonate, this difference may have a significant effect on the solubility of actinides. As an example, the FMT code (Novak 1996; Babb and Novak 1997; Wang 1998; Xiong et al. 2005) was used to calculate the solubility of Am(III) in a 5.6 m (5 M, molarity) NaCl solution in equilibrium with the brucite-hydromagnesite assemblage (Table 7). As shown in Table 7, if the Gibbs free energy of formation of brucite from Helgeson et al. (1978) was used, which was adopted in the SUP database of EQ3/6 code (Wolery 1992), the solubility-controlling phase for

Table 6 Fugacity of CO₂ gas buffered by the assemblage of brucite and hydromagnesite (5424) at 25°C by using different Gibbs free energy of formation of brucite

Buffer assemblage	Buffer reaction	log f_{CO_2} ^a
Brucite–hydromagnesite (5424)	$5 \text{ Mg(OH)}_2(\text{s}) + 4\text{CO}_2(\text{g}) = \text{Mg}_5(\text{CO}_3)_4(\text{OH})_2 \cdot 4\text{H}_2\text{O}(\text{s})$	-4.83 ^b
	$5 \text{ Mg(OH)}_2(\text{s}) + 4\text{CO}_2(\text{g}) = \text{Mg}_5(\text{CO}_3)_4(\text{OH})_2 \cdot 4\text{H}_2\text{O}(\text{s})$	-5.48 ± 0.24^c

^a In all calculations, thermodynamic data of CO₂(gas) and H₂O(l) are from CODATA (Cox et al. 1989), and the data of hydromagnesite (5424) are from Robie and Hemingway (1995)

^b The Gibbs free energy of formation of brucite is from Helgeson et al. (1978)

^c The Gibbs free energy of formation of brucite is from this study; the uncertainty of log f_{CO_2} is calculated from the uncertainty in Gibbs free energy of formation of brucite estimated in this study

Table 7 Predicted solubility of Am(III) in a 5.6 m (5 M) NaCl solution in equilibrium with brucite-hydromagnesite (5424) at different values of the Gibbs free energy of formation of brucite

Source of $\Delta_f G_{298.15, \text{brucite}}^\circ$	Solubility-controlling phase for Am(III)	Predicted solubility of Am(III)		
Helgeson et al. (1978)	AmOHCO ₃	Am(CO ₃) ₃ ³⁻ : 1.08×10^{-7} m		
		Am(CO ₃) ₂ ⁻ : 1.36×10^{-8} m		
		Am(CO ₃) ₄ ⁵⁻ : 1.34×10^{-8} m		
		Am(OH) ₂ ⁺ : 9.36×10^{-9} m		
		AmCO ₃ ⁺ : 1.99×10^{-10} m		
		Am(OH) ₃ ⁰ : 1.51×10^{-10} m		
		AmOH ²⁺ : 2.33×10^{-11} m		
		Am ³⁺ : 1.49×10^{-13} m		
		AmCl ²⁺ : 2.35×10^{-15} m		
		AmCl ₂ ⁺ : 9.52×10^{-17} m		
		ΣAm(III): 1.45×10^{-7} m		
		This study	Am(OH) ₃	Am(CO ₃) ₃ ³⁻ : 1.39×10^{-8} m
				Am(CO ₃) ₂ ⁻ : 1.99×10^{-9} m
Am(CO ₃) ₄ ⁵⁻ : 1.53×10^{-9} m				
Am(OH) ₂ ⁺ : 1.33×10^{-8} m				
AmCO ₃ ⁺ : 3.28×10^{-11} m				
Am(OH) ₃ ⁰ : 5.58×10^{-10} m				
AmOH ²⁺ : 1.18×10^{-11} m				
Am ³⁺ : 2.77×10^{-14} m				
AmCl ²⁺ : 4.34×10^{-16} m				
AmCl ₂ ⁺ : 1.78×10^{-17} m				
ΣAm(III): 3.14×10^{-8} m				

Am(III) would be AmCO₃OH(s) at the f_{CO_2} ($10^{-4.83}$ bars) buffered by the assemblage brucite-hydromagnesite (5424). In contrast, if the Gibbs free energy of formation of brucite from this study is used, the solubility-controlling phase would be Am(OH)₃(s) at the f_{CO_2} ($10^{-5.48 \pm 0.24}$ bars) buffered by the assemblage brucite-hydromagnesite (5424). Furthermore, the solubility of Am(III) in the former case is higher than that in the latter case by a factor of 4.6 (Table 7).

5 Summary

This study recommends that the solubility constant for the brucite dissolution reaction as written in Eq. 4 be 17.05 ± 0.2 (2σ), and the standard Gibbs energy of formation of brucite be -832.3 ± 1.1 (2σ) kJ mol⁻¹.

Acknowledgments Sandia National Laboratories is a multiprogram laboratory operated by Sandia Corporation, a Lockheed Martin Company, for the United States Department of Energy's National Nuclear Security Administration under Contract DE-AC04-94AL85000. This research is funded by WIPP programs administered by the Office of Environmental Management (EM) of the U.S. Department of Energy. My thanks are due to Nathalia Chadwick, Kelsey Mae Davis, and Veronica Gonzales, for their laboratory assistance. The author wishes to thank two journal reviewers for their insightful and thorough reviews, and to thank Dr. Frank Millero, the Associate Editor, for his editorial efforts.

References

- Altmairer M, Metz V, Neck V, Müller R, Fanghänel T (2003) Solid-liquid equilibria of Mg(OH)₂(cr) and Mg₂(OH)₃Cl·4H₂O(cr) in the system Mg–Na–H–OH–Cl–H₂O at 25°C. *Geochim Cosmochim Acta* 67(19):3595–3601. doi:[10.1016/S0016-7037\(03\)00165-0](https://doi.org/10.1016/S0016-7037(03)00165-0)
- Babb SC, Novak CF (1997) User's manual for FMT version 2.3: A computer code employing the Pitzer Activity Coefficient Formalism for calculating thermodynamic equilibrium in geochemical systems to high electrolyte concentrations [addendum included]. ERMS# 243037. Sandia National Laboratories, WIPP Records Center, Carlsbad, NM
- Babb SC, Novak CF, Moore RC (1996) WIPP PA (Waste Isolation Pilot Plant Performance Assessment) user's manual for NONLIN, version 2.0. ERMS# 230740. Sandia National Laboratories, WIPP Records Center, Carlsbad, NM
- Brown PL, Drummond SE Jr, Palmer DA (1996) Hydrolysis of magnesium (II) at elevated temperatures. *J Chem Soc, Dalton Trans* 14:3071–3075. doi:[10.1039/dt9960003071](https://doi.org/10.1039/dt9960003071)
- Busey RH, Mesmer RE (1978) Thermodynamic quantities for ionization of water in sodium-chloride media to 300°C. *J Chem Eng Data* 23(2):175–176. doi:[10.1021/jc60077a025](https://doi.org/10.1021/jc60077a025)
- Ciavatta L (1980) The specific interaction theory in evaluating ionic equilibria. *Annali di Chimica* 70(11–1): 551–567
- Cox JD, Wagman DD, Medvedev VA (1989) CODATA key values for thermodynamics. Hemisphere Publishing Corporation, NY. Available at <http://www.codata.org/resources/databases/key1.html> (5/12/07)
- Felmy AR (1990) GMIN: A computerized chemical equilibrium model using a constrained minimization of the Gibbs free energy. PNL-7281. Pacific Northwest National Laboratory, Richland, WA
- Giauque WF, Archibald RC (1937) The entropy of water from the third law of thermodynamics. The dissociation pressure and calorimetric heat of the reaction Mg(OH)₂ = MgO + H₂O: The heat capacities of Mg(OH)₂ and MgO from 20 to 300 K. *J Am Chem Soc* 59:561–569. doi:[10.1021/ja01282a039](https://doi.org/10.1021/ja01282a039)
- Guillaumont R, Fanghänel T, Fuger J, Grenthe I, Neck V, Palmer DA et al (2003) Update on the chemical thermodynamics of Uranium, Neptunium, Plutonium, Americium and Technetium. Elsevier, Amsterdam
- Gurvich LV, Veyts IV, Alcock CB (1994) Thermodynamic properties of individual substances. Vol 3. B, Al, Ga, In, Tl, Be, Mg, Ca, Sr, Ba and their compounds, part one: methods and computation. CRC Press, An Arbor, MI, p 707
- Harvie CE, Møller N, Weare JH (1984) The prediction of mineral solubilities in natural waters: the Na–K–Mg–Ca–H–Cl–SO₄–OH–HCO₃–CO₃–CO₂–H₂O system to high ionic strengths at 25°C. *Geochim Cosmochim Acta* 48(4):723–751. doi:[10.1016/0016-7037\(84\)90098-X](https://doi.org/10.1016/0016-7037(84)90098-X)
- Helgeson HC, Kirkham DH (1974) Theoretical prediction of the thermodynamic behavior of aqueous electrolytes at high pressures and temperatures. II. Debye–Hückel parameters for activity coefficients and relative partial molal properties. *Am J Sci* 274(10):1199–1261
- Helgeson HC, Delany JM, Nesbitt HW, Bird DK (1978) Summary and critique of the thermodynamic properties of rock-forming minerals. *Am J Sci* 278:1–229
- Hostetler PB (1963) The stability and surface energy of brucite in water at 25 C. *Am J Sci* 261:238–258

- Königsberger E, Königsberger LC, Gamsjäger H (1999) Low-temperature thermodynamic model for the system $\text{Na}_2\text{CO}_3\text{--MgCO}_3\text{--CaCO}_3\text{--H}_2\text{O}$. *Geochim Cosmochim Acta* 63(19–20):3105–3119. doi: [10.1016/S0016-7037\(99\)00238-0](https://doi.org/10.1016/S0016-7037(99)00238-0)
- Krumhansl JL, Panenguth HW, Zhang P-C, Kelly JW, Anderson HL, Hardesty JO (2000) Behavior of MgO as a CO_2 scavenger at the Waste Isolation Pilot Plant (WIPP), Carlsbad, New Mexico. *Mater Res Soc Symp Proc* 608:155–160
- McGee KA, Hostetler PB (1977) Activity-product constants of brucite from 10 to 90°C. *J Res US Geol Surv* 5:227–233
- Novak CF (1996) Development of the FMT chemical transport simulator: coupling aqueous density and mineral volume fraction to phase compositions. *J Contam Hydrol* 21(1–4):297–310. doi: [10.1016/0169-7722\(95\)00055-0](https://doi.org/10.1016/0169-7722(95)00055-0)
- Rai D, Felmy AR, Juracich SI, Rao FF (1995) Estimating the hydrogen ion concentration in concentrated NaCl and Na_2SO_4 electrolytes. SAND94-1949. Sandia National Laboratories, Albuquerque, NM
- Rard JA, Miller DG (1981) Isopiestic determination of the osmotic and activity coefficients of aqueous MgCl_2 solutions at 25°C. *J Chem Eng Data* 26(1):38–43. doi:[10.1021/je00023a014](https://doi.org/10.1021/je00023a014)
- Robie RA, Hemingway BS (1995) Thermodynamic properties of minerals and related substances at 298.15 K and 1 bar (10^5 pascals) pressure and at higher temperatures. United States Geological Survey Bulletin 2131
- Robie RA, Hemingway BS, Fisher JR (1978) Thermodynamic properties of minerals and related substances at 298.15 K and 1 bar (10^5 pascals) pressure and at higher temperatures. United States Geological Survey Bulletin 1452
- Schüssler W, Metz V, Kienzler B, Vejmelka P (2002) Geochemically based source term assessment for the Asse salt mine: comparison of modeling and experimental results (Abstract). Programs and Abstracts of Materials Research Society Annual Meeting at Boston, MA, p 713
- Wang Y (1998) WIPP PA validation document for FMT, version 2.4. Unpublished report. ERMS# 251587. Sandia National Laboratories, WIPP Records Center, Carlsbad, NM
- Wolery TJ (1992) EQ3/6, a software package for geochemical modeling of aqueous systems: package overview and installation guide (version 7.0). UCRL-MA-110662 Pt. I. Lawrence Livermore National Laboratory, Livermore, CA
- Wood SA, Palmer DA, Wesolowski DJ, Bénézeth P (2002) The aqueous geochemistry of the rare earth elements and yttrium. Part XI. The solubility of $\text{Nd}(\text{OH})_3$ and hydrolysis of Nd^{3+} from 30 to 290°C at saturated water vapor pressure with in-situ pHm measurement. In: Hellmann R, Wood SA (eds) Water–rock interactions, ore deposits, and environmental geochemistry: a tribute to David Crerar, Special Publication 7. The Geochemical Society, St. Louis, Missouri, USA, pp 229–256
- Xiong Y-L (2003) Revised thermodynamic properties of brucite determined by solubility studies and its significance to nuclear waste isolation, Abstracts with Programs. Geological Society of America Annual Meeting (Seattle, Washington, November 2–5, 2003) 35(6):102–103
- Xiong Y-L (2006) Estimation of medium effects on equilibrium constants in moderate and high ionic strength solutions at elevated temperatures by using specific interaction theory (SIT): interaction coefficients involving Cl^- , OH^- and Ac^- up to 200°C and 400 bars. *Geochem Trans* 7(4):1–19. doi: [10.1186/11467-4866-7-4](https://doi.org/10.1186/11467-4866-7-4)
- Xiong Y-L, Lord ACS (2008) Experimental investigations of the reaction path in the $\text{MgO--CO}_2\text{--H}_2\text{O}$ system in solutions with various ionic strengths, and their applications to nuclear waste isolation. *Appl Geochem* 23:1634–1659. doi:[10.1016/j.apgeochem.2007.12.035](https://doi.org/10.1016/j.apgeochem.2007.12.035)
- Xiong Y-L, Snider AC (2003) Experimental investigations of the reaction path in the system $\text{MgO--H}_2\text{O--CO}_2$ in concentrated brines at ambient temperature and ambient laboratory atmospheric CO_2 : Applications to the Waste Isolation Pilot Plant (Abstract). 2003 Radiochemistry Conference, July 13–16, 2003, Carlsbad, New Mexico, USA. Radiochemistry Society, Richland, WA. Available at <http://www.radiochemistry.org/abstracts/ExperimentalInvestigation.doc>, 5/17/05
- Xiong Y-L, Nowak EJ, Brush LH (2005) Predicting actinide solubilities in various solutions up to concentrated brines: the Fracture-Matrix Transport (FMT) code. *Geochim Cosmochim Acta* 69(10) (Supp. 1):A417